

LT-1 SAR SATELLITE CONSTELLATION FOR PERMAFROST DEFORMATION MONITORING ALONG THE TIBETAN PLATEAU ENGINEERING CORRIDOR

Xuefei Zhang¹, Tao Li¹, Xiang Zhang¹, Xiaoqing Zhou¹, Jing Lu¹, Xueguang Zhang²*

¹ Land Satellite Remote Sensing Application Center, Ministry of Natural Resources, Beijing, China - (zhangxf, lit, zhoxq, zhangx, luj)@lasac.cn

² Yunnan Construction Investment First Survey Design Co. Ltd., Kunming, China - 374253971@qq.com

KEY WORDS: LT-1, Permafrost, Tibetan Plateau, InSAR, Deformation monitoring, Engineering corridor.

ABSTRACT:

The Tibetan Plateau stands as one of China's largest middle and low latitude permafrost regions. However, the effects of global warming and human activities have led to permafrost thawing, inducing surface instability and posing significant threats to infrastructure and indigenous communities. The deployment of Lu Tan-1 (LT-1), China's premier L-band synthetic aperture radar (SAR) satellite constellation, offers a novel opportunity to assess these changes. This paper evaluates the deformation of critical engineering corridors, such as the Qinghai-Tibet Railway (QTR) and the Qinghai-Tibet Highway (QTH), utilizing time-series InSAR techniques with LT-1 SAR constellation data. We introduce both Stacking InSAR and a multi-baseline persistent scatterer multitemporal (MT-InSAR) method to enhance permafrost and engineering corridor deformation detection capabilities. Results obtained through the MT-InSAR approach reveal line-of-sight (LOS) deformation velocities of permafrost in the Beiluhe region ranging from -90 mm/y to approximately 70 mm/y, with an average velocity amplitude of 0.06 m/y. Differential displacement between alpine meadows and alpine deserts across the Beiluhe region is successfully discerned using LT-1 SAR data. Deformation velocities of QTR, QTH were found to be lower than that of permafrost, with average velocities of 0.027 m/y. These findings underscore the LT-1 SAR constellation's potential to serve as a valuable SAR data source for monitoring engineering corridor deformation within the Tibetan Plateau permafrost region.

1. INTRODUCTION

The Tibetan Plateau encompasses one of China's largest middle and low latitude permafrost regions, with over 50% of its area underlain by permafrost (Zhang et al., 2022). The region has witnessed extensive development initiatives such as the Western development strategy and the One Belt and One Road initiative, leading to the implementation of critical engineering projects like the Qinghai-Tibet Railway (QTR), the Qinghai-Tibet Highway (QTH), and infrastructure for oil pipelines and electric transmission lines (Zhang et al., 2019c; Zhang et al., 2019b). However, the combined impacts of global warming and human activities have accelerated permafrost thawing, resulting in surface instability and posing significant threats to infrastructure and indigenous communities. Certain segments of the QTR, QTH, and Power Transmission (PT) infrastructure have experienced destabilization due to the severe climate conditions and the freeze-thaw cycle of permafrost (Du et al., 2023). Consequently, precise measurement and monitoring of permafrost conditions along the Tibetan Plateau's engineering corridors are essential for environmental protection, understanding climate change dynamics, and mitigating cold-region hazards (Zhang et al., 2019c; Zhang et al., 2019b; Du et al., 2023).

With the continuous advancement of spaceborne Synthetic Aperture Radar (SAR) technology and the rapid progress in Interferometric SAR (InSAR) and Multi-temporal InSAR (MT-InSAR) techniques, there has been a significant enhancement in

the continuous monitoring of permafrost and engineering corridors like the QTH and the QTR using high-resolution SAR data. However, the effectiveness of InSAR is hindered by spatial-temporal decorrelation resulting from global temperature fluctuations, which impact the backscattering and phase characteristics of ground targets in these regions. The launch of the Lu Tan-1 (LT-1) satellite constellation, the first of its kind equipped with L-band SAR technology on January 26 and February 27, 2022, respectively, presents a novel opportunity. The satellite's monostatic formation mode offers new sources of high-resolution, long-wavelength, and high-revisit-frequency SAR data for monitoring deformations in QTR, QRH infrastructure corridors (Zhang et al., 2023; Li et al., 2023b). Despite this, the capacity and application effectiveness of LT-1 SAR data for monitoring engineering corridor deformations over permafrost regions using MT-InSAR techniques remain unexplored.

This paper addresses this gap by acquiring eight scenes of Stripmap1 pursuit monostatic formation (PMF) data, comprising five scenes from LT-1A and three scenes from LT-1B, spanning from March 2023 to January 2024 over typical engineer corridors in the Beiluhe region. Leveraging the developed MT-InSAR method, we successfully captured the temporal-spatial deformation characteristics of alpine meadows and alpine deserts. Additionally, we analyzed the spatial deformation characteristics of the QTR and QRH corridors with high-resolution SAR data.

* Corresponding author

2. STUDY AREA AND DATASET

2.1 Study Area

The study area is situated in the Beiluhe region, south of Qinghai province (see Figure 1a). This region falls within a warm continuous permafrost zone characterized by prevalent seasonal frozen soil. Elevations in the area range from 4400 to 5455 meters (as depicted in Figure 1) (Zhang et al., 2019a). According to data from the Beiluhe Weather Station, the average annual precipitation stands at approximately 369.8 mm/year, with over 90% of it occurring between May and September (Yin et al., 2017). The QTR, QTH and High voltage towers located in high-altitude regions are notably influenced by the permafrost environment (Figure 2).

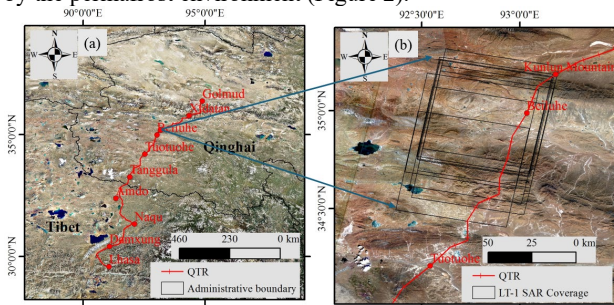


Figure 1. The study area and the LT-1 SAR coverage over the study area.

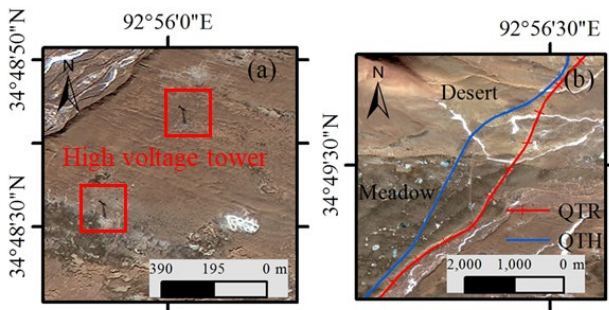


Figure 2. An example of engineering corridors in the study area.

2.2 Dataset

The LT-1 constellation represents China's pioneering SAR satellite constellation dedicated to deformation monitoring. Comprising two identical satellites, namely LT-1A and LT-1B, these satellites share the same design parameters. LT-1A was successfully launched on January 26, 2022, followed by the launch of LT-1B on February 27, 2022. The LT-1 constellation serves two essential formations. The first formation is known as the helix bistatic formation (HBF), where the satellites orbit each other to provide digital surface model (DSM) products. The second is the pursuit monostatic formation (PMF), wherein the satellites follow one another to offer deformation products (Li et al., 2023a). After the successful satellite launch, from February to December 2022, the satellites primarily operated in the HBF mode, continuously capturing data across China to produce DSM data products. Subsequently, the data transitioned to the PMF mode. For a single satellite, the LT-1's repeat orbit is 8 days, while it reduces to 4 days when two satellites work in tandem. LT-1 operates on the L-band system with a wavelength of approximately 23.5 cm, and azimuth and range pixel spacing of 1.57 m × 1.66 m (Li et al., 2023b).

The LT-1 SAR makes full use of the characteristics of the long L-band radar's wavelength and penetrating ability in vegetated areas, which can provide longwave SAR data with wide coverage, a high density of measurement points, and a high frequency of repeated observations for deformation monitoring of rock glacier. In this study, we acquired a total of 8 Stripmap1 PMF data scenes. These scenes collectively covered the study area (Figure 1b), enabling us to generate the deformation of permafrost engineer corridors. The spatial baseline combinations used in this is shown in the Figure 3.

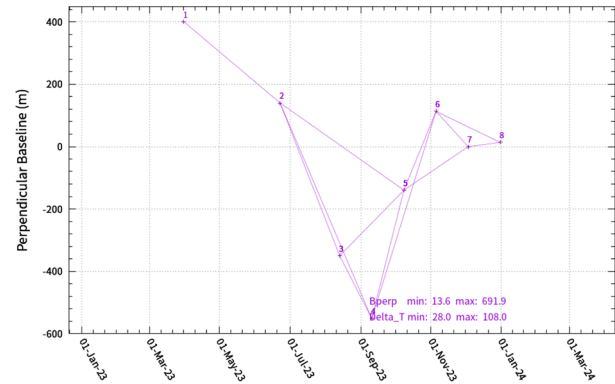


Figure 3. The spatial-temporal interferometric combinations of selected LT-1 SAR data.

3. METHODS

The methodology of this paper mainly includes SAR processing, Stacking InSAR processing, and multi-baseline persistent scatterer (PS) InSAR processing. The overall processing chain is illustrated in Figure 4.

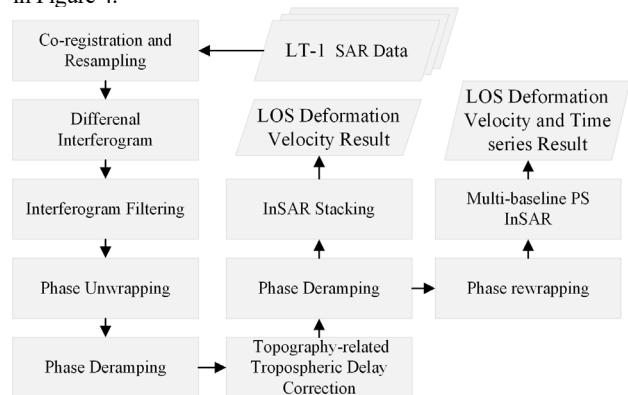


Figure 4. Flowchart of the proposed method.

3.1 InSAR processing

The InSAR processing of the images involved several steps, encompassing preprocessing tasks such as interferogram network selection, co-registration, generation of differential interferogram phases, phase filtering, and phase unwrapping. Furthermore, phase correction was conducted, primarily addressing phase deramping and topography-related tropospheric delay correction. Specifically, this paper employed empirical phase-based methods and network deramping techniques to implement corrections for topography-related interferometric atmospheric phase delays and orbital errors, respectively.

3.2 Stacking InSAR

The Stacking technique computes the rate of phase deformation by averaging interference phases, resulting in the Line-Of-Sight (LOS) surface deformation rate (Xu et al., 2022). Generating deformation velocity data requires more than two images. Initially, a differential interferogram is created using a specified range of spatio-temporal baselines. Subsequently, this differential interferogram undergoes filtering, unwrapping, detrending, de-atmospheric correction, and geocoding. Finally, a weighted averaging method is applied to calculate the phase deformation rate, yielding the final product.

The benefit of the deformation rate product lies in its ease of acquisition and its moderate accuracy, which improves with the inclusion of more images. However, a drawback is that this product may obscure certain abrupt deformations when identifying regions that are continuously subsiding.

3.3 MT-InSAR

Firstly, we conducted a selection process to identify scatterers with a mean coherence exceeding 0.7 from all chosen interferograms (see Figure 3), specifically those with small baselines, which were designated as Persistent Scatterers (PS). Subsequently, we constructed a Delaunay triangulation network (DTN) using the selected PS points. This network facilitated the inversion of Line of Sight (LOS) deformation. The DTN played a crucial role in removing the atmospheric phase screen (APS) through phase differencing of adjacent pixels, under the assumption that the APS of adjacent pixels is similar. This step helped mitigate atmospheric effects from the rewrapped interferometric phase (Zhang et al., 2021).

Within the DTN network, the deformation gradients of interconnected arcs were resolved through the differential wrapped phase of connecting nodes. This was achieved using optimization techniques such as the Nelder-Mead, modified residue-signal ratio (RSR), and M-estimator algorithms (Zhang et al., 2021). Initially, long arcs with a spatial distance exceeding 400 meters were excluded to eliminate arcs with significant differences in APS. Subsequently, the relative deformation rate between nodes within the arcs of the DTN was determined by maximizing the absolute value of the temporal coherence (Zhang et al., 2019d). Once the relative parameters for each arc were resolved, the absolute deformation parameters for each monitoring point were integrated using network adjustment. This integration process was performed for the largest connected network using a ridge-estimator-based weighted least square approach.

Finally, the deformation time series of the monitoring points was retrieved through conventional Persistent Scatterer Interferometry (PSI) processing.

4. EXPERIMENTAL RESULTS AND ANALYSIS

4.1 Interferometric coherence of LT-1 over permafrost engineering corridors

To investigate the interferometry performance of LT-1 data over the permafrost region of engineer corridors, we generated the interferometric coherence of LT-1 data with temporal baselines in different seasons. As shown in the Figure 5, LT-1 SAR data demonstrate good temporal coherence preservation capability in both alpine meadow areas and alpine desert areas. LT-1 SAR data from the same season exhibit better interferometric coherence. For instance, the interferometric coherence is highest in the summer months of June and August, and remains relatively good in November and January. This indicates that LT-1 SAR data

perform well in overcoming the influences of ice, snow, and vegetation changes. For LT-1 SAR data acquired in different seasons (such as March and June, August and November), the interferometric coherence slightly decreases but remains at a relatively high level. Areas of low coherence are mainly distributed in valley erosion zones. This indicates that surface changes caused by seasonal river variations are the primary reasons for interferometric decorrelation (Figure 5).

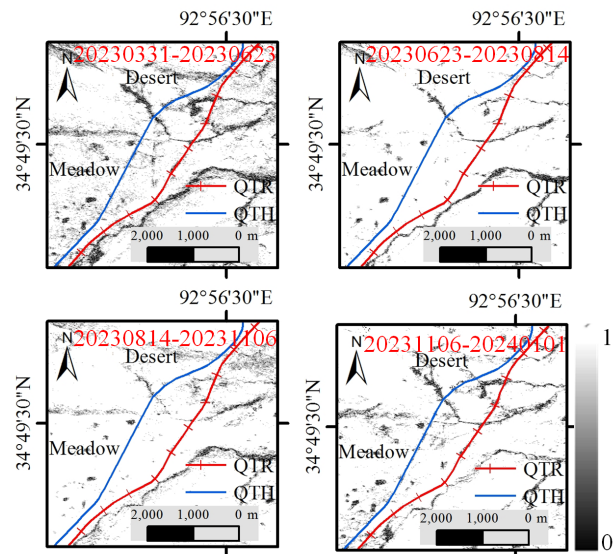


Figure 5. The interferometric coherence of LT-1 with different time intervals.

4.2 Stacking InSAR results

The LOS deformation velocities of the engineer corridors areas were obtained with the Stacking-InSAR method. Due to the thaw settlement characteristics exhibited by permafrost in summer and freeze expansion characteristics in winter, we conducted Stacking InSAR processing separately for all selected interferometric combinations, summer image interferometric combinations, and winter image interferometric combinations. This allowed us to obtain the overall deformation rate of the study area, as well as the summer thaw settlement rate and winter freeze expansion rate. The deformation rates of the engineering corridors in the study area, as indicated by Stacking InSAR results from all interferometric pairs, range from -0.22 to 0.56 m/y (Figure 6a,b). It can be observed that the deformation captured by Stacking InSAR processing of summer images mainly manifests as thaw settlement (deformation rate as negative values), while the deformation captured by winter images primarily appears as freeze expansion (deformation rate as positive values). The results indicate significant deformation differences between meadow and desert areas in both summer and winter (Figure 6c,d). This is attributed to the considerable difference in soil moisture content between meadow and desert areas. This deformation disparity has also been reflected in previous studies, which validates the accuracy of LT-1 SAR data in permafrost deformation monitoring applications. As shown in Figure 6, both the QTH and the QTR pass through areas with significant permafrost deformation, thus posing a considerable risk of frost-thaw disasters. Therefore, attention should be paid to the

frost-thaw disaster protection of transportation facilities in the Qinghai-Tibet Plateau.

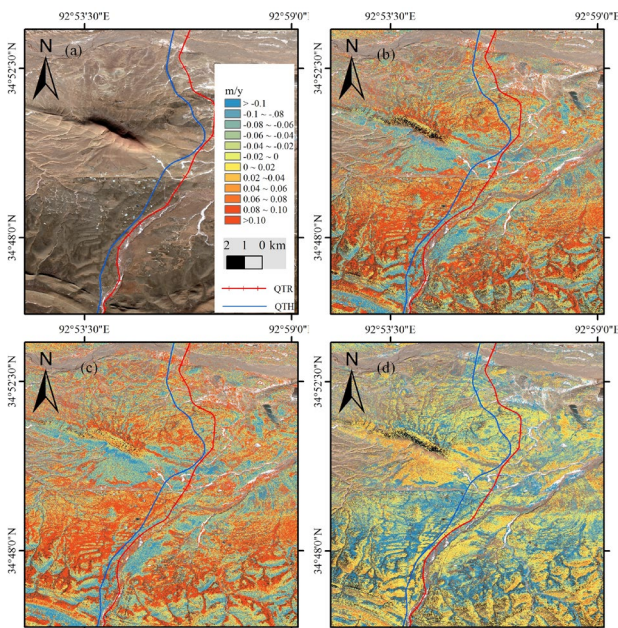


Figure 6. The Stacking InSAR deformation monitoring results. (a) The optical image of typical study area; (b) The Stacking InSAR LOS deformation velocity retrieved by the interferometric combinations of Figure 2; (c) and (d) are the Stacking InSAR LOS deformation velocity retrieved by the interferometric combinations with SAR imaged in summer (June-October) and in winter (October-January), respectively.

4.3 MT-InSAR results

The LOS deformation velocities and deformation time series of the permafrost engineer corridors in the study area were obtained from LT-1 SAR data with the proposed MT-InSAR method. Figure 7 showed the deformation velocities results. The deformation rates of the engineering corridors in the study area, as indicated by proposed MT-InSAR method from all interferometric pairs, range from -0.13 to 0.1 m/y, with an average velocity amplitude of 60 mm/y. Overall, the monitored values obtained from the MT-InSAR method are lower than those from the Stacking InSAR method. It is evident that the MT-InSAR results also captured the deformation rate differences between meadow and desert areas. However, there are certain discrepancies between these results and those obtained from Stacking InSAR. This is because Stacking InSAR technology relies on simple phase stacking principles, assuming linear temporal deformation and lacking optimized processing for residual phases. Therefore, the deformation rate results obtained by combining summer and winter images using Stacking InSAR may contain certain errors. However, it is important to note that Stacking InSAR results can still reflect regional deformation anomalies. Therefore, in situations where SAR data are limited, Stacking InSAR remains an effective approach for obtaining deformation rates. However, once the amount of SAR data meets the requirements for MT-InSAR application, MT-InSAR is preferred over Stacking InSAR due to its superior performance. Although the MT-InSAR method used in this study also relies on the assumption of basic linear deformation, it employs a multi-baseline network inversion algorithm in deformation calculation. Additionally, it separates residual phases during the time-series deformation

calculation process, allowing for the maximization of the temporal series characteristics and thus enhancing the accuracy of deformation estimation.

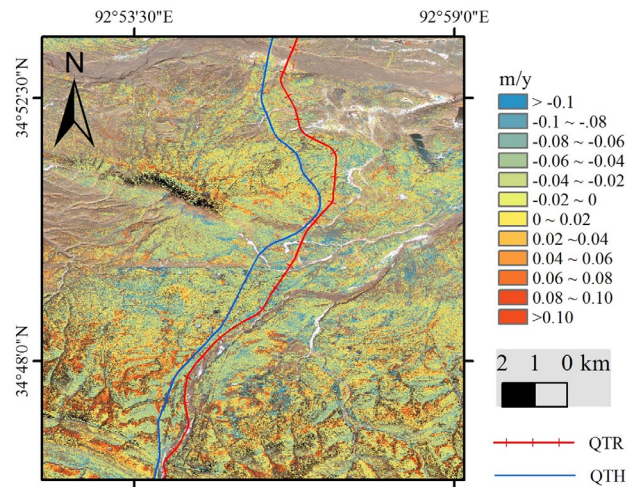


Figure 7. The MT-InSAR deformation monitoring results.

To reduce SAR data noise, this study employed a 2*2 multi-look operation in azimuth and range direction, resulting in a deformation rate product resolution of 5 meters. However, under these circumstances, monitoring linear features such as railways and highways posed significant challenges. In order to conduct a more detailed analysis of the spatial deformation characteristics within engineering infrastructure corridors of the study area. We established 50-meter-wide buffer zones around the QTH and QTR and extracted the deformation rates within these buffer zones (see Figure 8). Deformation velocities of the buffer region of QTR, QTH were found to be lower than that of full range of study area, with average velocities of 0.027 m/y. However, within the buffer zones, there are multiple areas with high deformation rates, which could potentially affect the structural integrity and safety of the roads. The LT-1 Stripmap Mode 1 data has approximately 1.5m pixel spacing in both the range and azimuth directions, making it suitable for monitoring linear features such as railways and highways. However, it requires single-look processing. Therefore, in the subsequent research, we will conduct a study on the application of Distributed Scatterer Time-Series InSAR based on single-look data. This aims to monitor the structural integrity of the QTH and QTR roads.

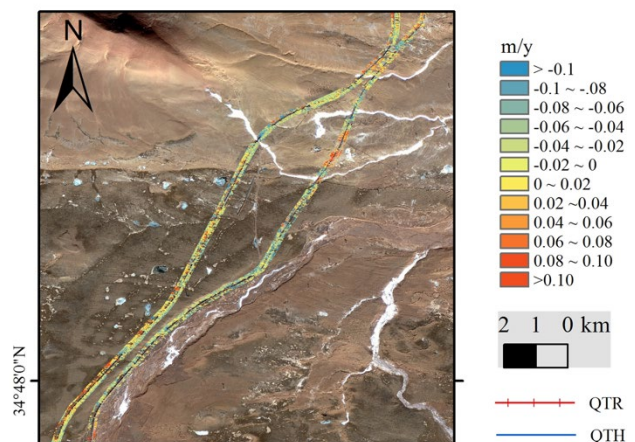


Figure 8. MT-InSAR deformation monitoring of QTR and QTH with a 50-meter buffer zone

The deformation time series results from MT-InSAR indicate clear seasonal variations in permafrost within the study area (Figure 9,10). This pattern correlates with the local temperature changes, effectively validating the accuracy of the study results. Figure 9 illustrates the temporal variation curves of typical monitoring points in the meadow and desert areas. It can be observed that the deformation magnitude in the desert area is lower than that in the meadow area. The meadow area exhibits distinct characteristics of thaw settlement in summer and freeze expansion in winter. The cumulative thaw settlement in the high cold meadow can reach 0.1m (Figure 9). The desert area appears relatively stable, showing less pronounced seasonal variations compared to the meadow area (Figure 9,10). The variation in deformation rates from March to June differs from that of other months due to the lack of additional images during this period. This period coincides with more drastic climate changes, leading to fluctuations in the freeze-thaw status and thus displaying anomalous rate patterns. Therefore, for better characterization of temporal variations in permafrost regions, denser observations are needed, especially during the period

from March to May and September to October when seasonal transitions occur. Higher frequency observations can enhance the capability to capture deformation patterns and improve monitoring accuracy.

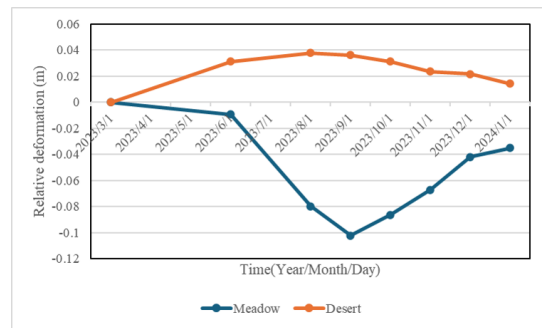


Figure 9. Time-series deformation of typical monitoring points.

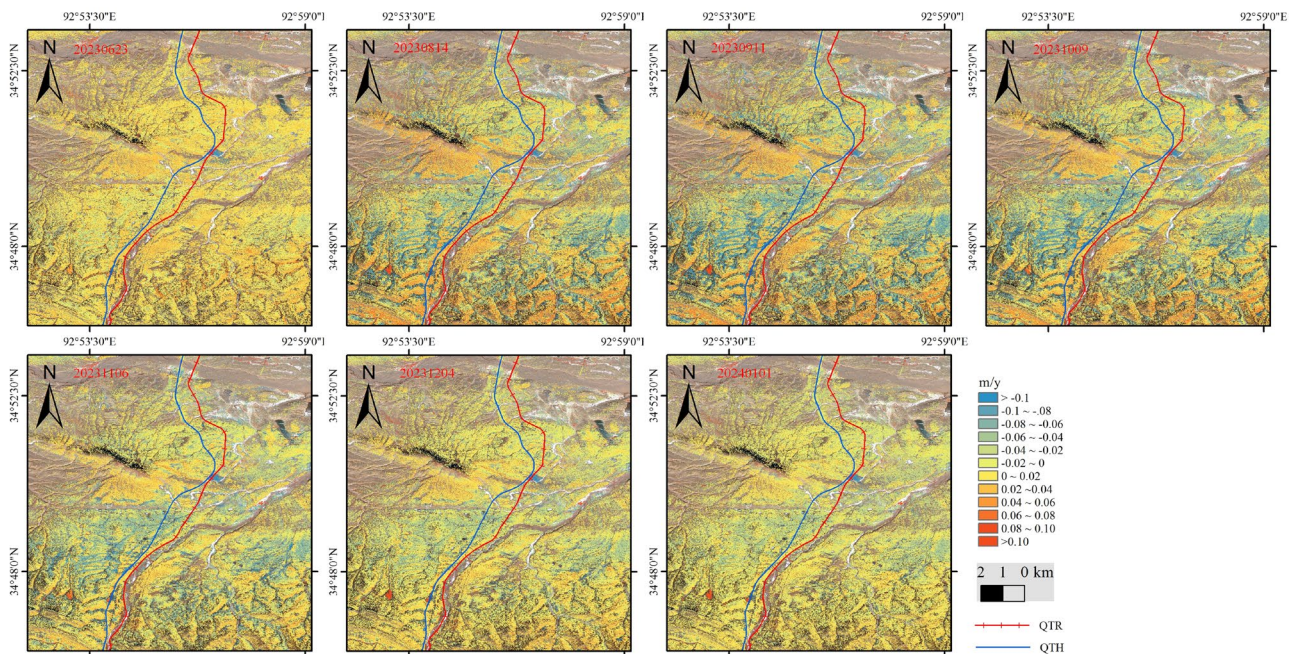


Figure 10. The Stacking InSAR deformation monitoring results.

5. CONCLUSIONS

This paper presents the first study on the application of time-series InSAR for engineering corridors in permafrost regions using LT-1 SAR satellite data. The main research findings are as follows:

- (1) By utilizing LT-1 SAR satellite data, this study demonstrates that with a relatively limited dataset (approximately 8 scenes), the time-series InSAR technique can effectively capture the spatiotemporal deformation characteristics of permafrost. This indicates the potential of LT-1 SAR satellite for monitoring deformations in permafrost regions.
- (2) The LT-1 SAR satellite exhibits excellent coherence preservation capabilities. Even under interferometric conditions spanning different seasons, the high cold meadows maintain a high level of coherence. This suggests that the LT-1 SAR satellite possesses strong resilience against vegetation and snow

interference. In permafrost regions, temporal decorrelation primarily arises from seasonal water erosion changes.

- (3) Extensive permafrost settlement and uplift around engineering facilities pose a significant risk of hazards such as thermokarst collapses. These hazards can easily lead to damage to engineering infrastructure, necessitating focused attention on these areas.

Despite the promising potential of LT-1 SAR satellite for permafrost deformation monitoring, and its high-resolution advantage, monitoring structural deformations of engineering facilities in permafrost regions using LT-1 SAR satellite under multi-look conditions remains challenging. It is necessary to utilize time-series InSAR techniques such as Distributed Scatterer Interferometry (DSI) under single-look conditions. Additionally, to obtain more detailed spatiotemporal deformation characteristics of permafrost and engineering facilities corridors, increasing satellite observation frequency and utilizing more data for monitoring are essential. In our

future research, we will continue to collect LT-1 SAR data and conduct more detailed studies on permafrost and engineering corridors areas.

6. ACKNOWLEDGEMENTS

This work was supported by the Young Scientists Fund of the National Natural Science Foundation of China (Grant NO. 42301160).

REFERENCES

Du, Q., Chen, D., Li, G., Cao, Y., Zhou, Y., Chai, M., Wang, F., Qi, S., Wu, G., Gao, K., and Li, C.: Preliminary Study on InSAR-Based Uplift or Subsidence Monitoring and Stability Evaluation of Ground Surface in the Permafrost Zone of the Qinghai–Tibet Engineering Corridor, China, *Remote Sensing*, 15, 10.3390/rs15153728, 2023.

Li, H., Li, B., Li, Y., and Duan, H.: The Stability Analysis of Mt. Gongga Glaciers Affected by the 2022 Luding MS 6.8 Earthquake Based on LuTan-1 and Sentinel-1 Data, *Remote Sensing*, 15, 10.3390/rs15153882, 2023a.

Li, T., Tang, X., Zhang, X., Zhang, X., Lu, J., Qiao, X., Chen, T., and Zhu, N.: First Application Demonstrations Of Lu Tan-1 SAR Satellites, 2023 SAR in Big Data Era (BIGSAR DATA), 20-22 Sept. 2023, 1-4, 10.1109/BIGSAR DATA59007.2023.10294711.

Xu, Y., Li, T., Tang, X., Zhang, X., Fan, H., and Wang, Y.: Research on the Applicability of DInSAR, Stacking-InSAR and SBAS-InSAR for Mining Region Subsidence Detection in the Datong Coalfield, *Remote Sensing*, 14, 10.3390/rs14143314, 2022.

Yin, G., Niu, F., Lin, Z., Luo, J., and Liu, M.: Effects of local factors and climate on permafrost conditions and distribution in Beiluhe basin, Qinghai-Tibet Plateau, China, *Science of the Total Environment*, 581, 472-485, 2017.

Zhang, X., Li, T., Zhang, X., Zhou, X., and Lu, J.: A Feasibility Study of LT-1 SAR Satellite for Permafrost Deformation Monitoring, 2023 SAR in Big Data Era (BIGSAR DATA), 20-22 Sept. 2023, 1-4, 10.1109/BIGSAR DATA59007.2023.10294951.

Zhang, X., Feng, M., Zhang, H., Wang, C., Tang, Y., Xu, J., Yan, D., and Wang, C.: Detecting Rock Glacier Displacement in the Central Himalayas Using Multi-Temporal InSAR, *Remote Sensing*, 13, 10.3390/rs13234738, 2021.

Zhang, X., Zhang, H., Wang, C., Tang, Y., Zhang, B., Wu, F., Wang, J., and Zhang, Z.: Time-Series InSAR Monitoring of Permafrost Freeze-Thaw Seasonal Displacement over Qinghai-Tibetan Plateau Using Sentinel-1 Data, 10.3390/rs11091000, 2019a.

Zhang, Z., Wang, M., Wu, Z., and Liu, X.: Permafrost Deformation Monitoring Along the Qinghai-Tibet Plateau Engineering Corridor Using InSAR Observations with Multi-Sensor SAR Datasets from 1997-2018, *Sensors (Basel)*, 19, 10.3390/s19235306, 2019b.

Zhang, Z., Fan, P., Liu, X., Wang, M., Wang, C., and Zhang, H.: Structural Health and Stability Assessment of Qinghai–Tibet Power Transmission Line with Time-Series InSAR Using X-Band

Terrasar Data, IGARSS 2019 - 2019 IEEE International Geoscience and Remote Sensing Symposium, 28 July-2 Aug. 2019, 2107-2110, 10.1109/IGARSS.2019.8899899.

Zhang, Z., Lin, H., Wang, M., Liu, X., Chen, Q., Wang, C., and Zhang, H.: A Review of Satellite Synthetic Aperture Radar Interferometry Applications in Permafrost Regions: Current status, challenges, and trends, *IEEE Geoscience and Remote Sensing Magazine*, 10, 93-114, 10.1109/MGRS.2022.3170350, 2022.

Zhang, Z., Wang, M., Liu, X., Wang, C., Zhang, H., Tang, Y., and Zhang, B.: Deformation Feature Analysis of Qinghai–Tibet Railway Using TerraSAR-X and Sentinel-1A Time-Series Interferometry, *IEEE Journal of Selected Topics in Applied Earth Observations and Remote Sensing*, 12, 5199-5212, 10.1109/jstars.2019.2954104, 2019d.